

# Identification and validation of key non-coding RNAs and mRNAs using co-expression network analysis in pre-eclampsia

Jing He, MM<sup>a</sup>, Kang Liu, MM<sup>a</sup>, Xiaohong Hou, MM<sup>b</sup>, Jieqiang Lu, MD<sup>b,\*</sup> 

## Abstract

Pre-eclampsia (PE) is a common complication of pregnancy, associated with maternal and fetal morbidity and mortality. In this study, we aimed to explore important long non-coding RNAs (lncRNAs) and their possible mechanisms in PE.

GSE60438 expression profile including 25 PE samples and 23 normal samples were obtained from gene expression omnibus (GEO) database. After normalization with betaqn package in R, differentially expressed lncRNAs (DElncRNAs) and mRNAs (DEmRNAs) were identified using the limma package. Gene Ontology (GO) and Kyoto encyclopedia of genes and genomes (KEGG) pathway were analyzed using DAVID 6.7 and GSEA 3.0. lncRNAs-mRNAs coexpression was implemented using weighted gene co-expression network analysis (WGCNA). MicroRNAs linked with these DElncRNAs and DEmRNAs were predicted and a competitive endogenous RNA (ceRNA) network was built.

A total of 53 DElncRNAs and 301 DEmRNAs were identified between control and PE samples. These DEmRNAs were enriched into pathways such as protein digestion and absorption, osteoclast differentiation. WGCNA constructed a lncRNA-mRNA coexpression network, among which *SUMO1P3*, *NACAP1*, *NCF1C*, *ANXA2P1*, *GTF2IP1*, *NAPSB*, *OR7E37P* were hub genes. ceRNA network was constructed together with microRNAs (miRNAs), and functional analysis indicated cellular membrane and sugar binding were involved in PE progression. Five lncRNAs *ANXA2P1*, *GTF2IP1*, *NACAP1*, *NCF1C* and *OR7E37P* were successfully validated in our clinical specimens.

The DElncRNAs, including *ANXA2P1*, *GTF2IP1*, *NACAP1*, *NCF1C* and *OR7E37P* might play important roles in PE. However, the exact mechanism of these lncRNAs in prediction and diagnosis of PE should be further explored.

**Abbreviations:** ANXA2P1 = annex in A2 pseudogenes, ceRNA = competitive endogenous RNA, DEGs = differentially expressed genes, DElncRNAs = differentially expressed lncRNAs, DEmRNAs = differentially expressed mRNAs, FC = fold change, GEO = gene expression omnibus, GSEA = gene set enrichment analysis, GO = gene ontology, KEGG = kyoto encyclopedia of genes and genomes, lncRNAs = long non-coding RNAs, MAD = median absolute deviation, miRNAs = microRNAs, NES = normalized enrichment score, PCC = Pearson correlation coefficient, PE = pre-eclampsia, OPG = osteoprotegerin, SUMO1P3 = Small ubiquitin-like modifier 1 pseudogene 3, WGCNA = weighted gene co-expression network analysis.

**Keywords:** preeclampsia, weight gene co-expression network analysis, predictive clinical biomarker

Editor: Roxana Covali.

This study was approved by the ethic committee of Shanxi Dayi Hospital.

The datasets used and analyzed in the current study are available from (GEO) database (<https://www.ncbi.nlm.nih.gov/geo/>) with accession number of GSE60438.

The authors have no funding and conflicts of interests to disclose.

The datasets generated during and/or analyzed during the current study are available from the corresponding author on reasonable request.

<sup>a</sup> Department of Obstetrics and Gynecology, Shanxi Bethune Hospital, Shanxi Medical University, Taiyuan, Shanxi, <sup>b</sup> Department of Obstetrics and Gynecology, The 2nd Affiliated Hospital of Wenzhou Medical University, Wenzhou, Zhejiang, PR China.

\* Correspondence: Jieqiang Lu, Department of Obstetrics and Gynecology, The 2nd Affiliated Hospital of Wenzhou Medical University, 306 Hualongqiao Road, Wenzhou 325000, Zhejiang, PR China (e-mail: jieqianglu666@163.com).

Copyright © 2021 the Author(s). Published by Wolters Kluwer Health, Inc. This is an open access article distributed under the terms of the Creative Commons Attribution-Non Commercial License 4.0 (CCBY-NC), where it is permissible to download, share, remix, transform, and buildup the work provided it is properly cited. The work cannot be used commercially without permission from the journal.

How to cite this article: He J, Liu K, Hou X, Lu J. Identification and validation of key non-coding RNAs and mRNAs using co-expression network analysis in pre-eclampsia. *Medicine* 2021;100:14(e25294).

Received: 6 December 2020 / Received in final form: 3 March 2021 / Accepted: 5 March 2021

<http://dx.doi.org/10.1097/MD.00000000000025294>

## 1. Introduction

Preeclampsia (PE) is characterized by new onset hypertension with other maternal organ dysfunction and fetal growth restriction.<sup>[1]</sup> As a highly variable and heterogeneous syndrome, PE is often associated with new-onset pretension, thrombocytopenia, impaired liver function, renal insufficiency, pulmonary edema, and cerebral disturbances.<sup>[2]</sup> It is estimated that 2% to 8% of pregnancies are affected by PE, which is evaluated to cause over 5000 maternal deaths worldwide per year and is considered as the leading cause of maternal and morbidity and mortality.<sup>[3]</sup> Delivery of the fetus and placenta is the only known cure for PE.<sup>[4]</sup>

The pathogenesis of PE is involved abnormal placentation and the development syndrome, but the exact underlying pathogenesis is largely unknown.<sup>[5]</sup> In recent years, long non-coding RNAs (lncRNAs) have been found play crucial roles in many diseases. Based on high-throughput techniques, several lncRNAs that might play important roles in PE have been identified in recent years. For example, He et al revealed that lncRNAs including *LOC284100*, *LOC391533*, and *CEACAMP8* were aberrantly expressed in PE and might contribute to PE pathogenesis.<sup>[6]</sup> Long et al found lncRNA *RP11-465L10.10* associated with the MMP9 gene was downregulated in PE patients.<sup>[7]</sup> Tong et al identified lncRNAs *HK2P1*, *BNIP3P1*, and *PGK1P1* were core regulatory

genes in PE.<sup>[8]</sup> In addition, microRNAs (miRNAs) have been reported as biomarkers in many diseases including cancer, cardiovascular disease, and diabetes mellitus.<sup>[9]</sup> Up-regulation of circulating miR-516-5p, miR-517-5p, miR-520a-5p, miR-525, and miR-526a is observed in PE.<sup>[10]</sup> Increasing evidence suggested that lncRNA might function as miRNA spongers to regulate expression of target genes, which was termed as “competitive endogenous (ceRNA)”. Although aberrantly expressed mRNAs, lncRNAs, and miRNAs have been identified extensively in PE, the lncRNA-miRNA-mRNA network-ceRNA network has been poorly reported.

Weighted Gene Co-expression Network Analysis (WGCNA) draws gene expression network, in which pairs of genes were identified based on the correlated expression across samples.<sup>[11]</sup> WGCNA analysis has been widely applied in recent years to identify core genes involved in disease occurrence and development.<sup>[12,13]</sup> In this study, we identified the differentially expressed genes (DEGs), including differentially expressed mRNAs (DEmRNAs) and differentially expressed lncRNAs (DElncRNAs) between PE samples and normal samples. WGCNA was implemented on DEGs to construct coexpression network. Gene ontology (GO) and Kyoto encyclopedia of genes and genomes (KEGG) pathway analyses were performed for the DEmRNAs. Additionally, the hub lncRNAs were verified in clinical samples. Our research provided newly candidate genes that are important in PE and might have potential to serve as biomarkers in PE diagnosis.

## 2. Materials and methods

### 2.1. Data source

The raw data of expression profile of GSE60438 based on platforms of GPL6884 and GPL10558 were obtained from the gene expression omnibus (GEO) database (<https://www.ncbi.nlm.nih.gov/geo/>). This dataset included genome-wide transcriptome sequencing data on 65 normotensive and 60 PE patients and was contributed by Yong et al.<sup>[14]</sup> The sequencing data based on the platform of GPL6884, which included 48 samples from 25 PE samples and 23 normal samples, were extracted for further analysis.

### 2.2. Identification of DEGs

The sequencing data were downloaded and genes were annotated into mRNAs, and lncRNAs based on GENCODE database (release 26). Data were normalized with betaqn package in R (version 1.16.0; <https://www.rdocumentation.org/packages/watermelon/versions/1.16.0/topics/betaqn-exprmethy450-methods>). Further, differential gene expression analysis was implemented using the limma package (version 3.10.3) in R. The resulting *P* value was adjusted using Benjamini & Hochberg method. The mRNAs with adjusted *P* value <.05 and |log fold change (FC)| >0.5 and the lncRNAs with adjusted *P* value <.05 were regarded as differentially expressed.

### 2.3. Functional enrichment analysis

The GO was performed using DAVID version 6.7 (<https://david.ncifcrf.gov/>) and visualized by GO plot in R.<sup>[15]</sup> KEGG pathway enrichment was implemented using Gene set enrichment analysis version 3.0 (GSEA) with the adjusted *P* value <.05 (<https://www.genome.jp/kegg/>). The pathway with normalized

enrichment score (NES) >0 represented the activated pathway while pathway with NES <0 was suppressed.

### 2.4. Weighted correlation network analysis

WGCNA (version 1.61) in R was used to construct coexpression network. The input genes were first filtered by removing those with median absolute deviation (MAD) <0.01 and among the later 25% MAD. The genes with missing value were also removed. Then, the Pearson correlation coefficient (PCC) between each pair of genes was calculated, then the adjacency function was defined, and module partitioning was performed based on the threshold of minimal module size of 30 genes. In addition, correlation between gene modules and clinical phenotypes including age, gestational age, and infant weight was calculated and clinical phenotype-related modules were identified.

### 2.5. Construction and functional annotation of ceRNA network

The PCCs between DElncRNAs and differentially expressed mRNAs were calculated using psych package (version v1.8.12; <https://www.rdocumentation.org/packages/psych/versions/1.8.12>) in R based on corr.test method. Coexpressed pairs were screened based on criteria of adjusted *P* value <.05 and  $|r| \geq 0.75$  and coexpression network was visualized using Cytoscape (version 3.7.0).

MiRNAs that could target the coexpressed lncRNAs and mRNAs were predicted from starbase database (<http://starbase.sysu.edu.cn/starbase2/>) and mirwalk database (<http://mirwalk.umm.uni-heidelberg.de/>). LncRNA-mRNA pairs regulated by the same miRNAs were integrated into lncRNA-miRNA-mRNA network and visualized by Cytoscape. The function of the mRNAs in these RNAs network was analyzed for GO and KEGG pathway enrichment using DAVID with *P* value <.05.<sup>[16]</sup>

### 2.6. Validation of hub lncRNAs in the ceRNA network by qRT-PCR

The decidua basalis was obtained from 5 PE patients and 5 normotensive maternal women who were delivered in the department of Obstetrics and Gynecology, Shanxi Bethune

**Table 1**  
The sequences of primers for qRT-PCR.

Gene	Direction	Sequence (5–3)
SUMO1P3	Forward	ACTGGCACCCCATCTCTTTG
SUMO1P3	Reverse	CATCAGGGCCAATTCGCAAG
NACAP1	Forward	GCTGAGACAGGGTCTGGAAC
NACAP1	Reverse	CTGGACTTGTGCGGTACCT
NCF1C	Forward	CAGTCATGGGGACACCTTC
NCF1C	Reverse	TCCTGCCATTTACCAGGAA
ANXA2P1	Forward	AATGGGCATGGGACTCAAG
ANXA2P1	Reverse	ATGGGGAGCACCATTCTGG
GTF2IP1	Forward	CGAAAGTTGAAAAAGCTGTCGC
GTF2IP1	Reverse	ATGCCATCAACCACCACACA
NAPSB	Forward	TCATCCAGTTTGCTCAGGGT
NAPSB	Reverse	TCGAAGACGGTCACATACGC
OR7E37P	Forward	ACAATGCTGGGTGTTGGTTTAC
OR7E37P	Reverse	TTCTGTGGGTCTGTAGAGATTG
GAPDH	Forward	TGACAACCTTGGTATCGTGGAGG
GAPDH	Reverse	AGGCAGGGATGATGTTCTGGAGAG

Hospital. This study was approved by the ethic committee of Shanxi Dayi Hospital.

Total RNA of decidua basalis was extracted using TRIzol reagent (Thermo Fisher). Qualified RNA was reverse-transcribed into cDNA using the Prime Script RT master mix (TaKaRa, Shiga, Japan). The amplification was performed on ViiA7 Real-time PCR System (Thermo Fisher) using Power SYBR Green PCR master (Thermo Fisher). The relative expression level of lncRNA was calculated using the  $2^{-\Delta\Delta C_t}$  method using GAPDH as internal control. The primers used are listed in Table 1.

**2.7. Statistical analysis**

Each reaction of qRT-PCR was repeated 3 times and data were represented as mean  $\pm$  standard deviation. Comparisons between

groups were conducted by student's *t* test in Graphpad Prism 5.0. *P* < .05 was regarded as significant.

**3. Results**

**3.1. DEGs identification in PE samples**

A total of 14337 mRNAs and 11091 lncRNAs were included in the dataset of GSE60438. Among them, 96 upregulated mRNAs and 205 downregulated mRNAs as well as 26 upregulated ncRNAs and 27 downregulated ncRNAs were filtered out (Fig. 1A and B). Hierarchical clustering analysis was performed and the top 10 up-regulated and down-regulated genes were illustrated in heatmap (Fig. 1C).

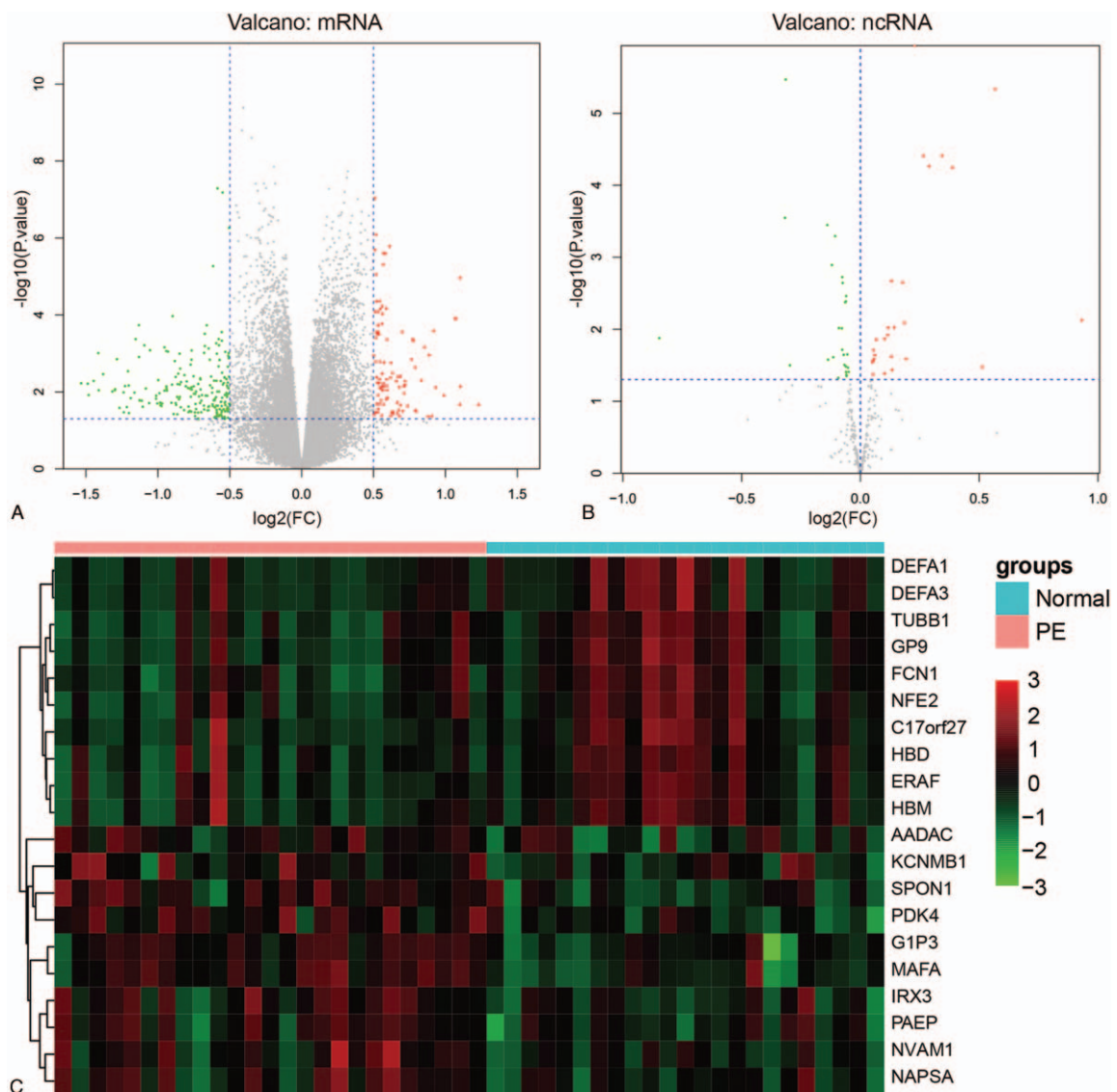


**Figure 1.** Differentially expressed genes (DEGs) identification between pre-eclampsia and normal samples. (A) Volcano plot of differentially expressed mRNAs (DEmRNAs). The vertical dotted lines represent  $|\log_2 \text{fold change (FC)}| > 0.5$  and the horizontal lines represent *P* value < .05. Red spots represent up-regulated mRNAs and green spots represent down-regulated mRNAs in PE samples compared with normal samples. (B) Volcano plot of differentially expressed ncRNAs. Red spots represent up-regulated ncRNAs and green spots represent down-regulated ncRNAs in PE samples compared with normal samples. (C) Hierarchical clustering of top 10 expressed DEGs. The heatmap demonstrated the top 10 up-regulated and down-regulated genes in descending order by  $|\log_2(\text{FC})|$ .



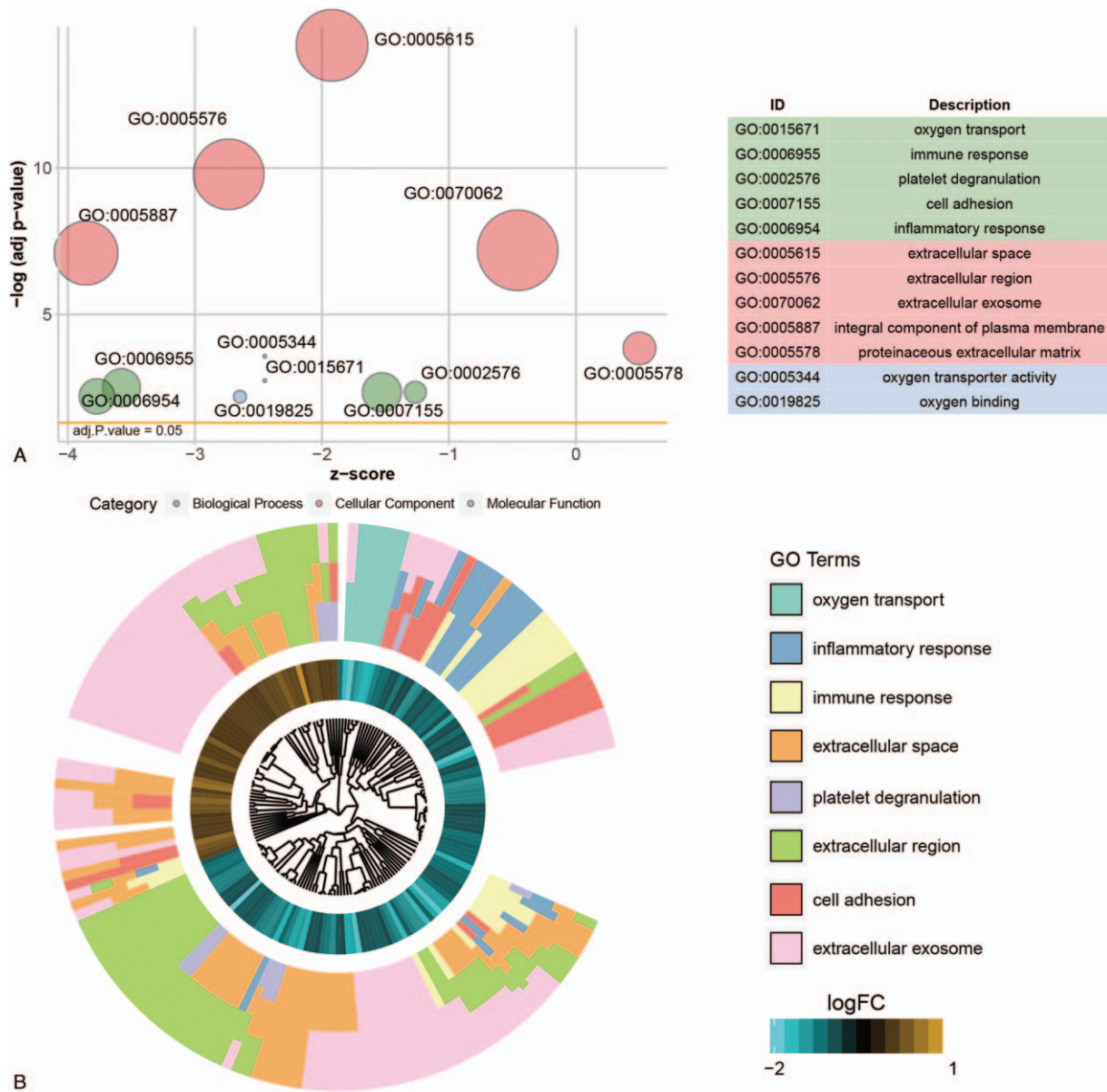


**Figure 2.** Gene ontology (GO) enrichment analysis. (A) The bubble plot of GO terms. X-axis represents the Z-score and y-axis represents the negative log adjusted P value. The area of the bubble positively correlates with the gene numbers in the indicated term. The green bubbles represent the GO terms enriched in biological process; the pink bubbles represented the GO terms enriched in cellular component and the blue bubbles represented the molecular function term. (B) GO cluster of genes in the top 8 GO term grouped by their expression level.

### 3.2. Functional annotation of DEMRNAs

To explore the biological function of these DEMRNAs, GO and KEGG pathway enrichment analyses were performed (Fig. 2). As a result, 25 GO terms including 10 biological process terms, 13 cellular component terms and 2 molecular function terms were significantly enriched ( $P < .05$ ). The DEMRNAs were mainly enriched in biological processes including “oxygen transport” ( $P$  value =  $1.32E-06$ ), “immune response” ( $P$  value =  $6.88E-06$ ), “inflammatory response” ( $P$  value =  $1.32E-05$ ), “cell adhesion” ( $P$  value =  $6.63E-06$ ), “angiogenesis” ( $P$  value =  $2.28E-05$ ), and “platelet degranulation” ( $P$  value =  $8.52E-05$ ). The DEMRNAs were mainly located on “extracellular space” ( $P$  value =  $2.97E-17$ ),

“integral component of plasma membrane” ( $P$  value =  $1.47E-09$ ), “proteinaceous extracellular matrix” ( $P$  value =  $3.31E-06$ ), “plasma membrane” ( $P$  value =  $7.74E-05$ ), and “cell surface” ( $P$  value =  $1.28E-04$ ). These results revealed that these genes functioned in cell-cell communication and interaction. “Oxygen transporter activity” and “oxygen binding” were the 2 significant enriched molecular function terms by DEMRNAs.

Next, KEGG pathway enrichment was performed and 85 significantly enriched pathways were identified. Among them, 15 pathways were activated ( $NES > 0$ ) and 70 pathways were suppressed ( $NES < 0$ ). Pathways such as “protein digestion and absorption,” “fatty acid degradation,” “valine/leucine and isoleucine degradation,” “glyoxylate and dicarboxylate metabo-

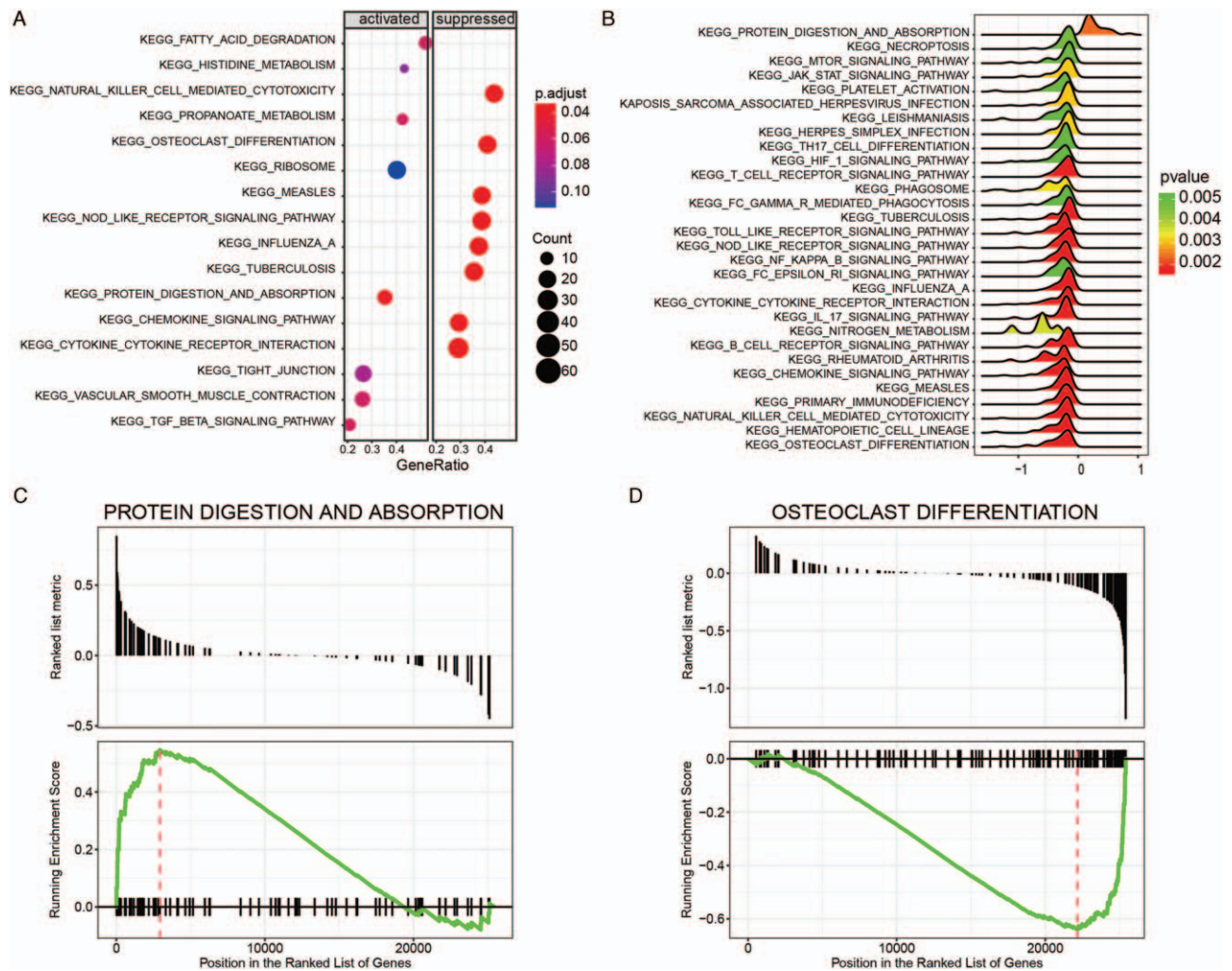


**Figure 3.** Gene set enrichment analysis of KEGG pathways. (A) Dot plot of dysregulated pathways in PE samples compared with normal samples. The color intensity of the nodes indicated KEGG pathways enriched degree. Horizontal axis indicated the gene ratio as the proportion of differential genes in the whole gene set. The size represented the number counts in a certain pathway. (B) Ridge plot of dysregulated pathways. The colored intensity of peaks indicated enrichment significance. (C) The most activated pathway of “protein digestion and absorption.” Normalized enrichment score (NES) was positive for most genes in “protein digestion and absorption.” (D) The most suppressed pathway of “osteoclast differentiation.” NES was negative for most genes in “osteoclast differentiation” pathway.

lism,” “histidine metabolism” were activated (Fig. 3A and B). The immune related pathways including “natural killer cell mediated cytotoxicity,” “primary immunodeficiency,” “rheumatoid arthritis,” “B cell receptor signaling pathway,” “T cell receptor signaling pathway,” “intestinal immune network for IgA production,” “chemokine signaling pathway,” “IL 17 signaling pathway,” “NF kappa B signaling pathway,” and “TNF signaling pathway” were significantly suppressed (Fig. 3A and B). “Protein digestion and absorption” pathway was the most significant active pathway (Fig. 3C). The “osteoclast differentiation pathway” was the most significantly suppressed one (Fig. 3D).

### 3.3. WGCNA analysis of DEGs

By integrating the clinical symptom and the gene expression data, the expression profile of 305 DEGs in 48 samples were obtained.

WGCNA analysis further filtered out 228 DEGs for further analysis. Most of these genes were significantly classified into 3 modules, including 131 genes in ME turquoise module, 60 genes in ME blue module, and 34 genes in ME brown module (Fig. 4A). Genes in the same module showed significant correlation, while revealed poor correlation other modules (Fig. 4A and 4B). Among the 3 identified modules, genes enriched in ME turquoise module showed higher degree, compared with those in the ME blue and ME brown modules. These data indicated that genes in ME turquoise demonstrated more function than genes in the other modules (Fig. 4C). In this network, high degree genes including *TMEM71*, *SELL*, *Rgr*, *RGS18*, *P2RY13*, *NALP12*, *MCEMP1*, *LST1*, *LRG1*, and *LILRA2* were filtered out.

Clinical symptoms such as disease status, gestational age and infant weight showed great correlation with these 3 modules. However, maternal age did not reveal significant difference (Table 2).



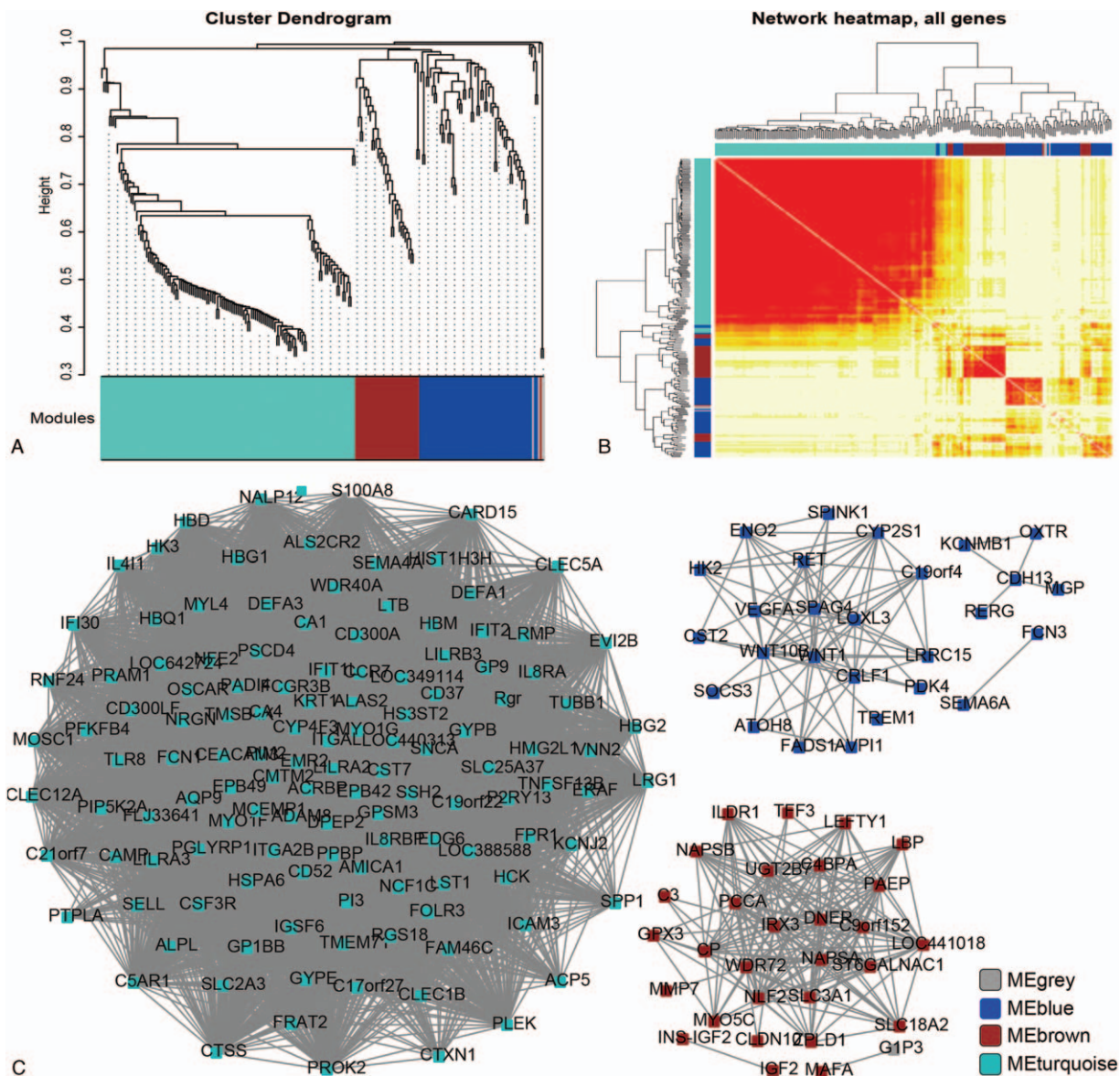


**Figure 4.** WGCNA analysis of DEGs. (A) Cluster dendrogram of DEGs in network. Different colors represented different modules. (B) Hierarchical clustering analysis of differently expressed genes. The color in the heatmap indicated correlated degree between the 2 genes. Genes in row and column were analyzed together. Deeper color represented the more correlation. (C) ncRNA-mRNA coexpression network construction. Blue: MEBLue module; brown: MEBrown module; turquoise: MEturquoise module.

### 3.4. Construction and functional annotation of ceRNA network

To further analyze the genes in the 3 modules, paired genes with adjusted *P* value <.05 and  $|r| \geq 0.75$  were calculated and a

lncRNA-mRNA coexpression network was constructed (Fig. 5). There were 74 nodes and 102 edges including 58 mRNAs and 16 ncRNAs. High connect nodes were identified such as *SUMO1P3*, *NACAP1*, *NCF1C*, *ANXA2P1*, *GTF2IP1*, *NAPSB*, and *OR7E37P*.

**Table 2**  
The correlation between clinical phenotype and WGCNA modules.

	module	disease	age	gestational age (weeks)	infant weight (g)
cor	MEBrown	0.4495985	-0.163577	-0.3600296	-0.3853923
	MEturquoise	-0.398738	0.0218055	0.3558121	0.5037802
	MEBlue	-0.555048	0.1298954	0.4023702	0.3802591
<i>P</i> value	MEBrown	1.35E-03	0.2665997	0.011953145	6.83E-03
	MEturquoise	5.00E-03	0.8830466	0.013065607	2.62E-04
	MEBlue	4.23E-05	0.3788831	0.004580631	7.68E-03

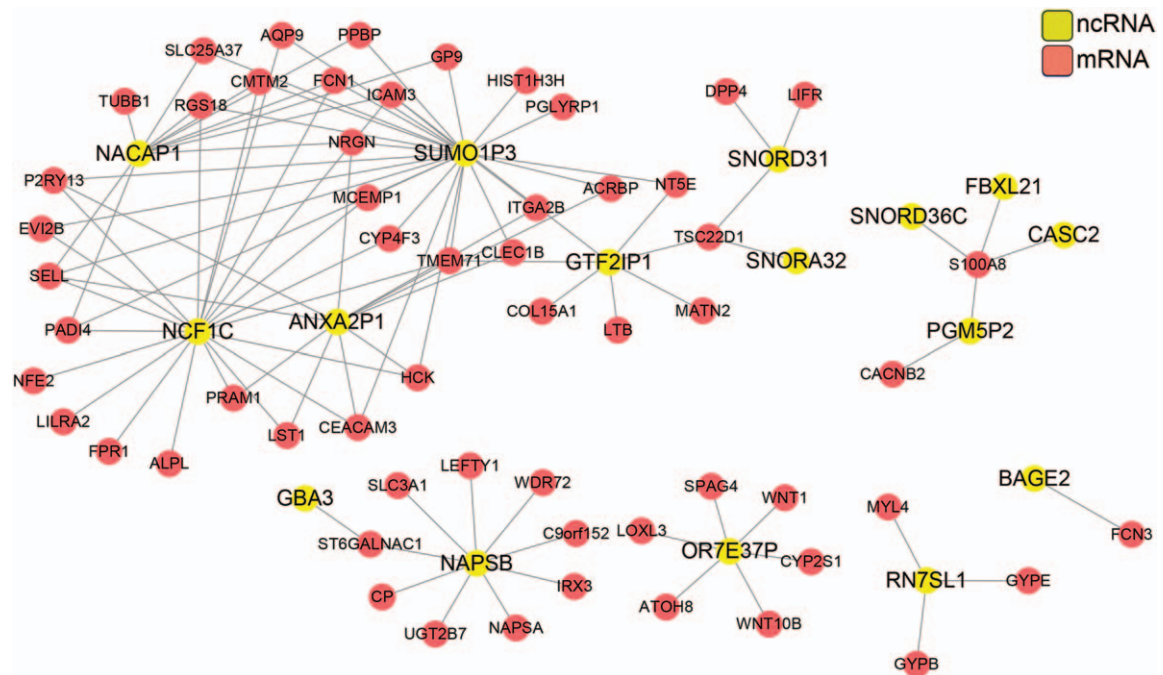


**Figure 5.** ncRNA-mRNA network construction for the genes from the 3 modules. Gene pairs were chosen using correlation ratio  $|r| \geq 0.75$  and adj.  $P$  value  $< .05$ . Red, mRNA; yellow, ncRNA.

We screened ncRNA-mRNA pairs regulated by a common miRNA, which was predicted from starbase and miRwalk databases. These ncRNA-mRNA pairs together with miRNAs were integrated into a ceRNA network including 25 mRNAs, 7

ncRNAs and 43 miRNAs (Fig. 6). Functional analysis of the network revealed that genes in this network were involved in molecular function of carbohydrate binding and sugar binding and were mostly located on cellular membrane (Table 3).

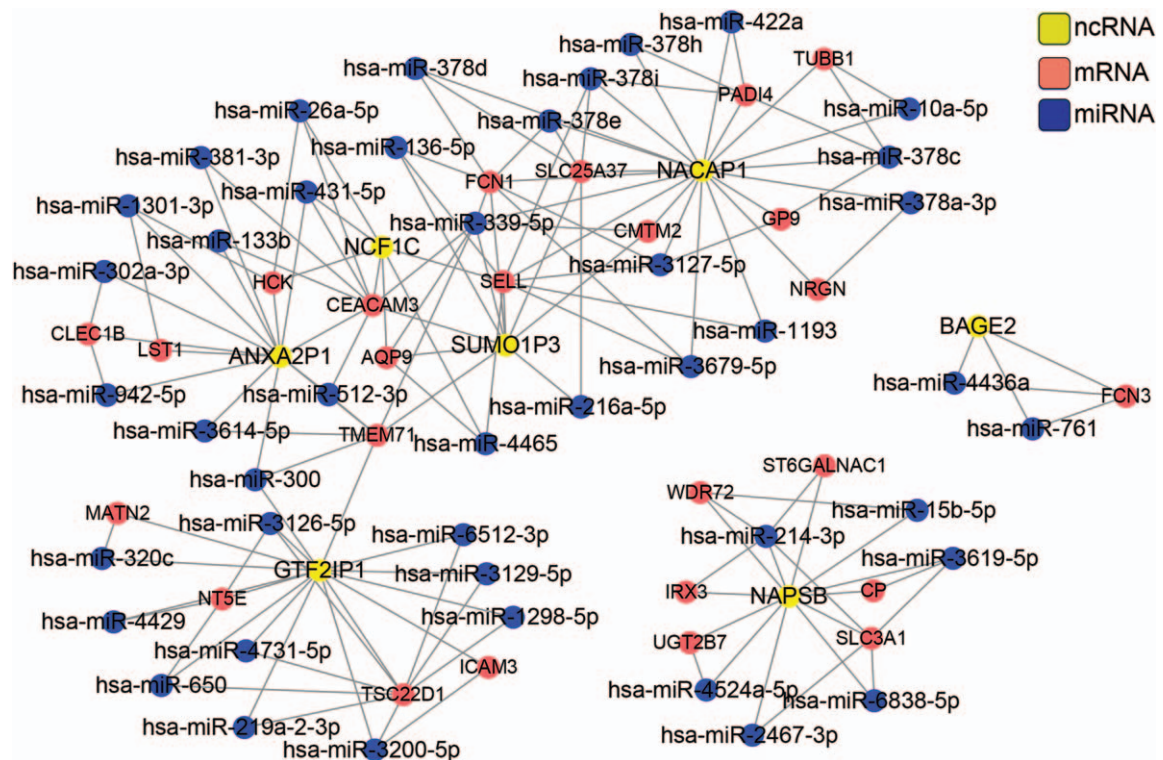


**Figure 6.** ceRNA network construction and functional analysis. Red, mRNA; yellow, ncRNA; blue, miRNA.



**Table 3**  
The enriched GO term from ceRNA network.

Category	ID	Description	P value
CC	GO:0031224	intrinsic to membrane	.00153
CC	GO:0031226	intrinsic to plasma membrane	.006676
CC	GO:0005887	integral to plasma membrane	.026502
CC	GO:0031225	anchored to membrane	.041611
CC	GO:0016021	integral to membrane	.046561
CC	GO:0044421	extracellular region part	.049485
MF	GO:0005529	sugar binding	.002708
MF	GO:0030246	carbohydrate binding	.014083

CC = cellular component, MF = molecular function.

**Table 4**  
Patient characteristics.

Patient characteristics	PE	Normotensive	P
Maternal age, years	30.6 ± 7.7	32.4 ± 4.6	0.67
Gestational age, weeks	33 ± 4.4	39 ± 4.8	0.0066
Infant birth weight, g	1862 ± 604.2	3482 ± 619.85	0.003
Systolic blood pressure, mmHg	156 ± 16.7	122.6 ± 4.4	0.0025
Diastolic blood pressure, mmHg	101.2 ± 11.0	75 ± 7.8	0.0025
Proteinuria, g/24h	3.2 ± 2.3	NA	NA

**3.5. Validation of hub lncRNAs in the ceRNA network by qRT-PCR**

The 7 lncRNAs in the ceRNA network included *SUMO1P3*, *NACAP1*, *NCF1C*, *ANXA2P1*, *GTF2IP1*, *NAPSB*, and *OR7E37P*. Differential expression analysis revealed that *SUMO1P3* (adjusted *P* value = .002074, logFC = 0.266), *NACAP1* (adjusted *P* value = .002074, logFC = 0.266), *ANXA2P1* (adjusted *P* value = .000408, logFC = 0.567569), *GTF2IP1* (adjusted *P* value = .002151, logFC = 0.387), and *NAPSB* (adjusted *P* value = .007509, logFC = 0.932425) were upregulated in PE patients while *NCF1C* (adjusted *P* value = .0131776, logFC = -0.847) and *OR7E37P* (adjusted *P* value

= .031679, logFC = -0.29648) were downregulated. We further verified expression of these 7 lncRNAs in 5 PE patients and 5 normotensive maternal women. The characteristics of these women are displayed in Table 4. There was no significant difference between the 2 groups on maternal age (*P* > .05). The gestational age, infant birth weight, systolic blood pressure and diastolic blood pressure were significantly different between these 2 groups (*P* < .05).

qRT-PCR results are displayed in Figure 7. The differential expression of the upregulated lncRNAs *ANXA2P1*, *GTF2IP1*, *NACAP1* and the downregulated lncRNAs *NCF1C*, *OR7E37P* were successfully validated in our clinical specimens (*P* < .05). However, there is no significantly difference between control and PE patients on small ubiquitin-like modifier 1 pseudogene 3 (*SUMO1P3*) and *NAPSB* expression (*P* > .05).

**4. Discussion**

PE is defined as hypertension associated with one or more new-onset conditions including proteinuria, renal insufficiency, liver involvement, neurological complications, haematological complications, or uteroplacental dysfunction.<sup>[5]</sup> Various pathways have been implicated in the pathogenesis. In this study, we found DEGs were enriched in oxygen transport, immune response, inflammatory response, cell adhesion, angiogenesis, and platelet degranulation function. These genes were involved in immune related pathways and many other signaling pathways. Next, WGCNA analysis was performed to explore the hub genes combined with clinical syndrome. Further analysis revealed that disease, gestational age and infant weight were closely associated with identified modules. We identified 7 hub lncRNAs: *SUMO1P3*, *NACAP1*, *NCF1C*, *ANXA2P1*, *GTF2IP1*, *NAPSB* and *OR7E37P*. Five of these hub lncRNAs, including *ANXA2P1*, *GTF2IP1*, *NACAP1*, *NCF1C*, and *OR7E37P* were successfully validated in our clinical specimens.

The placental and maternal dysfunctions contribute to the pathogenesis of PE. Several genetic, angiogenic and other pathways have been showed in PE. Trophoblast invasion impairment would lead to imbalance between pro- and anti-angiogenic factors.<sup>[17,18]</sup> Endothelial cells count a lot in

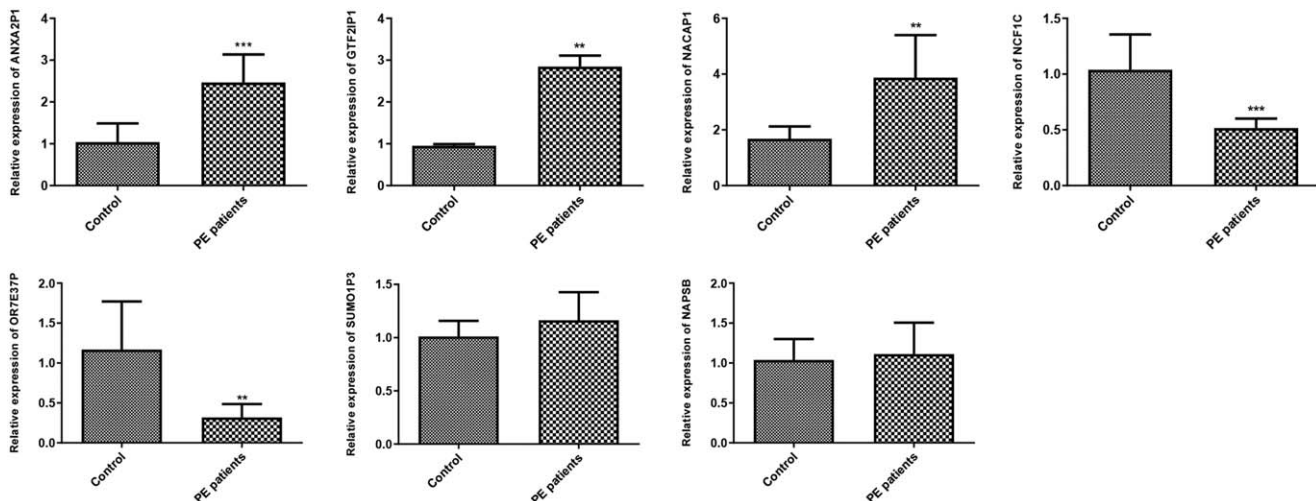


**Figure 7.** Validation of hub lncRNAs in the ceRNA network by qRT-PCR. Comparisons between groups were conducted by student's *t* test in Graphpad Prism 5.0. \*\* indicated *P* < .01, \*\*\* indicated *P* < .001.



inflammatory response, which would up-regulated the cytokines and adhesion factors secretion in PE.<sup>[19,20]</sup> Additionally, placental oxygenation, redox and immune tolerance have also been involved in PE.<sup>[21,22]</sup> Our research is consistent with previous studies that DEGs enriched in oxygen transport, immune response, inflammatory response, cell adhesion and angiogenesis, platelet degranulation function. All these pathways have been implicated in PE. Notably, the “osteoclast differentiation” was found to be significantly suppressed in PE. During pregnancy, bone turnover increases significantly in order to meet the demands from the fetus.<sup>[23]</sup> Evidences suggested that bone metabolism is altered in hypertensive pregnancies compared with normotensive pregnancies and bone resorption is increased and bone formation is decreased in PE patients.<sup>[24,25]</sup> Vitoratos et al demonstrated that PE patients exhibit higher OPG (osteoprotegerin) levels, a key factor in inhibiting bone resorption, which might be compatible with lower bone turnover.<sup>[26]</sup> Consistent with these studies, our study supports that bone turnover in PE was suppressed in PE compared with control pregnancies.

Various investigations have been implemented for possible biomarkers in PE. Angiogenic factors emerged as important biomarkers in PE. Imbalance of these factors located in the central position of pathogenesis of PE. The expression of PIGF, sFLT1, and sENG differs significantly between women with PE and normotensive pregnancies. The ratio of sFLT1 to PIGF and PIGF to sENG is characterized with good performance in prediction.<sup>[27–30]</sup> In addition, ICAM-1 and VCAM-1 in endothelial dysfunction, cell free fetal DNA marker HYP2, NK cells in immune reaction, ROS in oxidative stress and other biomarkers including ADAM-12, PAPP-A, and PP-13 have been implicated their clinical function in PE.<sup>[31–34]</sup>

In our research, 7 hub genes: *SUMO1P3*, *NACAP1*, *NCF1C*, *ANXA2P1*, *GTF2IP1*, *NAPSB*, and *OR7E37P* were identified as the diagnostic biomarker in prediction of PE. All these genes including protein coding gene and non-coding gene have not been reported before.

Small ubiquitin-like modifier 1 pseudogene 3 (*SUMO1P3*) is a pseudogene-expressed lncRNA which served as the oncogenic lncRNA in many kinds of human malignancy. Differently expressed *SUMO1P3* has been reported in gastric cancer, non-small cell lung cancer, bladder cancer and hepatocellular carcinoma, which revealed its diagnostic function.<sup>[35–39]</sup> *ANXA2P1* is differently expressed pseudogenes between glioblastomas and normal control tissues.<sup>[40]</sup> Deletion breakpoints mapping to *GTF2IP1* is associated with Williams–Beuren syndrome.<sup>[41]</sup> Over-expressed *NAPSB* has been identified in carcinoma of the uterine cervix and this result indicated its correlation with *CACX*.<sup>[42]</sup> To our surprise, the function of *NACAP1*, *NCF1C* and *OR7E37P* have yet to be reported. All these genes were firstly reported in pathology of PE, thus providing the underlying clinically predictive significance. Other points we should pay attention to are all these identified genes were pseudogenes and these remind us that pseudogenes could be new biomarkers in PE progress.

There are some limitations in this study. First, though 5 of these hub lncRNAs, including *ANXA2P1*, *GTF2IP1*, *NACAP1*, *NCF1C*, and *OR7E37P* were successfully validated in our clinical specimens, the sample size is relatively small. Further studies involved in a large sample size are still warranted. Second, though the key lncRNAs involved in PE were identified, the exact mechanism of these lncRNAs involved in PE should be further studied.

In conclusion, we identified 355 DEGs between PE and normal samples. Functional analysis showed that immune pathway, inflammation pathway, and cell adhesion pathway were involved in development of PE. Further WGCNA analysis constructed ncRNA-mRNA network. Three modules were constructed and hub genes were filtered out. The hub ncRNAs combined with physical status might not only mediate the relationship between biological pathways, but also offer novel insights into the diagnosis and pathogenesis of PE. Combined with miRNAs, ceRNA network was constructed. Hub lncRNAs including *SUMO1P3*, *NACAP1*, *NCF1C*, *ANXA2P1*, *GTF2IP1*, *NAPSB*, and *OR7E37P* were identified and 5 lncRNAs *ANXA2P1*, *GTF2IP1*, *NACAP1*, *NCF1C*, and *OR7E37P* were successfully validated in our clinical specimens. However, further validation in a large sample size set and molecular mechanism of these key lncRNAs should be investigated in future.

### Author contributions

**Acquisition of data:** Xiaohong Hou

**Analysis and interpretation of data:** Jing He, Kang Liu

**Conceptualization:** Jing He.

**Data curation:** Kang Liu, Jieqiang Lu.

**Drafting the manuscript:** Jing He

**Formal analysis:** Jing He.

**Methodology:** Kang Liu, Xiaohong Hou, Jieqiang Lu.

**Project administration:** Jing He.

**Revision of manuscript for important intellectual content:** Jieqiang Lu

### References

- [1] Lowe SA, Bowyer L, Lust K, et al. SOMANZ guidelines for the management of hypertensive disorders of pregnancy 2014. *Aus New Zealand J Obstet Gynaecol* 2015;55:e1–29.
- [2] American College of Obstetricians and Gynecologists . Hypertension in pregnancy. Report of the American College of Obstetricians and Gynecologists’ task force on hypertension in pregnancy. *Obstet Gynecol* 2013;122:1122–31.
- [3] Steegers EAP, von Dadelszen P, Duvekot JJ, et al. Pre-eclampsia. *Lancet* 2010;376:631–44.
- [4] Cox AG, Marshall SA, Palmer KR, et al. Current and emerging pharmacotherapy for emergency management of preeclampsia. *Exp Opin Pharmacother* 2019;20:701–12.
- [5] Phipps EA, Thadhani R, Benzang T, et al. Pre-eclampsia: pathogenesis, novel diagnostics and therapies. *Nat Rev Nephrol* 2019;15:275–89.
- [6] He X, He Y, Xi B, et al. LncRNAs expression in preeclampsia placenta reveals the potential role of LncRNAs contributing to preeclampsia pathogenesis. *PLoS One* 2013;8:e81437.
- [7] Long W, Rui C, Song X, et al. Distinct expression profiles of lncRNAs between early-onset preeclampsia and preterm controls. *Clinica Chimica Acta* 2016;463:193–9.
- [8] Tong J, Zhao W, Lv H, et al. Transcriptomic profiling in human decidua of severe preeclampsia detected by RNA sequencing. *J Cell Biochem* 2018;119:607–15.
- [9] Creemers EE, Tijssen AJ, Pinto YM, et al. Circulating microRNAs: novel biomarkers and extracellular communicators in cardiovascular disease? *Circ Res* 2012;110:483–95.
- [10] Hromadnikova I, Kotlabova K, Ondrackova M, et al. Circulating C19MC microRNAs in preeclampsia, gestational hypertension, and fetal growth restriction. *Mediators Inflamm* 2013;2013:186041.
- [11] Giulietti M, Righetti A, Principato G, et al. LncRNA co-expression network analysis reveals novel biomarkers for pancreatic cancer. *Carcinogenesis* 2018;39:1016–25.
- [12] Huang T, Wang Y, Wang Z, et al. Weighted gene co-expression network analysis identified cancer cell proliferation as a common phenomenon during perineural invasion. *Oncotargets Ther* 2019;12:10361–74.
- [13] Xia WX, Zhang LH, Liu YW. Weighted gene co-expression network analysis reveals six hub genes involved in and tight junction function in

- pancreatic adenocarcinoma and their potential use in prognosis. *Genetic Testing Mol Biomarkers* 2019;23:829–36.
- [14] Yong HE, Melton PE, Johnson MP, et al. Genome-wide transcriptome directed pathway analysis of maternal pre-eclampsia susceptibility genes. *PLoS One* 2015;10:e0128230.
- [15] Walter W, SanchezCabo F, Ricote M. GOrplot: an R package for visually combining expression data with functional analysis. *Bioinformatics (Oxford, England)* 2015;31:2912–4.
- [16] Juhas M, Crook DW, Hood DW, et al. Secretion systems: tools of bacterial horizontal gene transfer and virulence. *Cell Microbiol* 2008;10:2377–86.
- [17] Lu F, Longo M, Tamayo E, et al. The effect of over-expression of sFlt-1 on blood pressure and the occurrence of other manifestations of preeclampsia in unrestrained conscious pregnant mice. *Am J Obstet Gynecol* 2007;196:396e391–396.e397.
- [18] Roberts JM, Rajakumar A. Preeclampsia and soluble fms-like tyrosine kinase 1. *J Clin Endocrinol Metab* 2009;94:2252–4.
- [19] Daniel Y, Kupfermanc MJ, Baram A, et al. Plasma soluble endothelial selectin is elevated in women with pre-eclampsia. *Hum Reprod* 1998;13:3537–41.
- [20] Henriksen T. The role of lipid oxidation and oxidative lipid derivatives in the development of preeclampsia. *Sem Perinatol* 2000;24:29–32.
- [21] Myatt L, Cui X. Oxidative stress in the placenta. *Histochem Cell Biol* 2004;122:369–82.
- [22] Rahimi Z, Malek-Khosravi S, Rahimi Z, et al. MTHFR C677T and eNOS G894T variants in preeclamptic women: contribution to lipid peroxidation and oxidative stress. *Clin Biochem* 2013;46:143–7.
- [23] Pitkin RM. Calcium metabolism in pregnancy and the perinatal period: a review. *Am J Obstet Gynecol* 1985;151:99–109.
- [24] Shaarawy M, Zaki S, Ramzi AM, et al. Feto-maternal bone remodeling in normal pregnancy and preeclampsia. *J Soc Gynecol Investig* 2005;12:343–8.
- [25] Anim-Nyame N, Sooranna SR, Jones J, et al. Biochemical markers of maternal bone turnover are elevated in pre-eclampsia. *BJOG* 2001;108:258–62.
- [26] Vitoratos N, Lambrinouadaki I, Rizos D, et al. Maternal circulating osteoprotegerin and soluble RANKL in pre-eclamptic women. *Eur J Obstet Gynecol Reprod Biol* 2011;154:141–5.
- [27] Kusanovic JP, Romero R, Chaiworapongsa T, et al. A prospective cohort study of the value of maternal plasma concentrations of angiogenic and anti-angiogenic factors in early pregnancy and midtrimester in the identification of patients destined to develop preeclampsia. *J Matern Fetal Neonatol* 2009;22:1021–38.
- [28] Kleinrouweler CE, Wiegerinck MMJ, Ris-Stalpers C, et al. Accuracy of circulating placental growth factor, vascular endothelial growth factor, soluble fms-like tyrosine kinase 1 and soluble endoglin in the prediction of pre-eclampsia: a systematic review and meta-analysis. *BJOG* 2012;119:778–87.
- [29] Chappell LC, Duckworth S, Seed PT, et al. Diagnostic accuracy of placental growth factor in women with suspected preeclampsia. *Circulation* 2013;128:2121–31.
- [30] Moore Simas TA, Crawford SL, Bathgate S, et al. Angiogenic biomarkers for prediction of early preeclampsia onset in high-risk women. *J Maternal-Fetal Neonatal Med* 2014;27:1038–48.
- [31] Grill S, Rusterholz C, Zanetti-Dällenbach R, et al. Potential markers of preeclampsia—a review. *Reprod Biol Endocrinol* 2009;7:70.
- [32] Lockwood CJ, Huang SJ, Chen CP, et al. Decidual cell regulation of natural killer cell-recruiting chemokines: implications for the pathogenesis and prediction of preeclampsia. *Am J Pathol* 2013;183:841–56.
- [33] Kim SY, Kim HJ, Park SY, et al. Early prediction of hypertensive disorders of pregnancy using cell-free fetal DNA, cell-free total DNA, and biochemical markers. *Fetal Diagn Ther* 2016;40:255–62.
- [34] McCarthy FP, Ryan RM, Chappell LC. Prospective biomarkers in preterm preeclampsia: a review. *Pregnancy Hypertens* 2018;14:72–8.
- [35] Mei D, Song H, Wang K, et al. Up-regulation of SUMO1 pseudogene 3 (SUMO1P3) in gastric cancer and its clinical association. *Med Oncol* 2013;30:709.
- [36] Li PF, Chen SC, Xia T, et al. Non-coding RNAs and gastric cancer. *World J Gastroenterol* 2014;20:5411–9.
- [37] Zhang Y, Li Y, Han L, et al. SUMO1P3 is associated clinical progression and facilitates cell migration and invasion through regulating miR-136 in non-small cell lung cancer. *Biomed Pharmacother* 2019;113:108686.
- [38] Tian C, Jin Y, Shi S. Long non-coding RNA SUMO1P3 may promote cell proliferation, migration, and invasion of pancreatic cancer via EMT signaling pathway. *Oncol Lett* 2018;16:6109–15.
- [39] Zhou Y, He P, Xie X, et al. Knockdown of SUMO1P3 represses tumor growth and invasion and enhances radiosensitivity in hepatocellular carcinoma. *Mol Cell Biochem* 2019;450:125–34.
- [40] Li S, Zou H, Shao YY, et al. Pseudogenes of annexin A2, novel prognosis biomarkers for diffuse gliomas. *Oncotarget* 2017;8:106962–75.
- [41] Bayés M, Magano LF, Rivera N, et al. Mutational mechanisms of Williams–Beuren syndrome deletions. *Am J Hum Genet* 2003;73:131–51.
- [42] Roychowdhury A, Samadder S, Das P, et al. Deregulation of H19 is associated with cervical carcinoma. *Genomics* 2020;112:961–70.